

Deep Copula Classifier: Theory, Consistency, and Empirical Evaluation

Agnideep Aich^{1*}, Ashit Baran Aich²

¹ Department of Mathematics, University of Louisiana at Lafayette,
Lafayette, LA, USA.

² Department of Statistics, Formerly of Presidency College,
Kolkata, India

Abstract

We present the Deep Copula Classifier (DCC), a class-conditional generative model that separates marginal estimation from dependence modeling using neural copula densities. DCC is interpretable, Bayes-consistent, and achieves excess-risk $O(n^{-r/(2r+d)})$ for r -smooth copulas. In a controlled two-class study with strong dependence ($|\rho| = 0.995$), DCC learns Bayes-aligned decision regions. With oracle or pooled marginals, it nearly reaches the best possible performance (accuracy ≈ 0.971 ; ROC-AUC ≈ 0.998). As expected, per-class KDE marginals perform less well (accuracy 0.873; ROC-AUC 0.957; PR-AUC 0.966). On the Pima Indians Diabetes dataset, calibrated DCC ($\tau=1$) achieves accuracy 0.879, ROC-AUC 0.936, and PR-AUC 0.870, outperforming Logistic Regression, SVM (RBF), and Naive Bayes, and matching Logistic Regression on the lowest Expected Calibration Error (ECE). Random Forest is also competitive (accuracy 0.892; ROC-AUC 0.933; PR-AUC 0.880). Directly modeling feature dependence yields strong, well-calibrated performance with a clear probabilistic interpretation, making DCC a practical, theoretically grounded alternative to independence-based classifiers.

Keywords: Deep Copula Classifier, Neural Copulas, Generative Classification, Feature Dependence, Bayes Consistency

1. Introduction

Classification, the assignment of labels based on features, is a key part of machine learning. Classical methods such as logistic regression (Cox, 1958), support vector machines (Cortes and Vapnik, 1995), and naive Bayes (McCallum and Nigam, 1998) work well in many cases but depend on certain assumptions. For example, naive Bayes assumes features are independent, linear discriminant analysis requires features to be Gaussian with the same covariance, and neural networks capture feature interactions through weight matrices rather than explicit probabilistic models.

In real-world situations, features often interact in complex, nonlinear ways. For example, financial indicators can move together in extreme ways that simple correlation does not capture (Embrechts, McNeil and Straumann, 2002). In medical diagnostics, biomarkers such as blood pressure and cholesterol may have nonlinear relationships that are important for predicting disease. If these interdependencies are ignored, classifier performance can suffer. Copulas address this issue by separating the marginal distributions from the dependence structure among variables (Sklar, 1959). While traditional parametric copulas like Gaussian, Clayton, and Gumbel,

*Corresponding author: Agnideep Aich, agnideep.aich1@louisiana.edu, ORCID: [0000-0003-4432-1140](https://orcid.org/0000-0003-4432-1140)

as well as newer Archimedean types (Aich, Aich and Wade, 2025), can model basic patterns, they struggle with high-dimensional data or more complex dependencies. Neural copulas (Ling, Fang and Kolter, 2020; Wilson and Ghahramani, 2010; Gordon et al., 2020) use deep learning to adapt and handle these challenges more effectively.

We address this gap with the Deep Copula Classifier (DCC). For each class, DCC models individual features using their marginal distributions and learns how features depend on each other using neural network parameterized copulas. This generative method enables measuring how features vary together, allowing classifiers to leverage these dependency patterns. Our theoretical contributions include the following:

1. **Novel Framework:** Integration of deep copulas into a class-conditional generative classifier.
2. **Consistency Proof:** DCC converges to Bayes-optimality under standard conditions.
3. **Rate Quantification:** $O(n^{-r/(2r+d)})$ excess risk for r -smooth copulas.
4. **Interpretability:** Direct inspection of learned copula dependencies.
5. **Extensions Roadmap:** High-dimensional, semi-supervised, and streaming adaptations.

We validate DCC with two studies using a single, fair protocol. All methods use identical fixed data splits. No hyperparameter tuning is performed (defaults only). A held-out calibration subset is used for Platt calibration for all models, including DCC. Models are fit on the training portion only, calibration is learned on the calibration subset, and a single evaluation is run once on the held-out test set.

- *Experiment 1 (synthetic dependence).* On correlated Gaussians with $|\rho| = 0.995$, DCC learns decision regions aligned with the Bayes boundary. With the same hyperparameters across marginal strategies, oracle and pooled marginals achieve near-ceiling performance (accuracy ≈ 0.971 , ROC–AUC ≈ 0.9975 , PR–AUC ≈ 0.9976). Per-class KDE marginals underperform due to finite-sample marginal estimation (accuracy 0.873, ROC–AUC 0.957, PR–AUC 0.966), highlighting the role of stable marginal estimation when dependence drives class separation.
- *Experiment 2 (PIMA).* On the Pima Indians Diabetes dataset, with per-class median imputation, mild per-class winsorization, fixed train/calibration/test splits, and shared Platt calibration, calibrated DCC with $\tau=1$ attains Accuracy = 0.879, ROC–AUC = 0.936, and PR–AUC = 0.870. Random Forest is strongest on Accuracy and PR–AUC (Accuracy = 0.892, ROC–AUC = 0.933, PR–AUC = 0.880), while DCC attains the highest ROC–AUC. Logistic Regression, SVM (RBF), and Gaussian Naïve Bayes trail DCC on ROC–AUC (0.855, 0.891, 0.861, respectively). Reliability curves show DCC and Logistic Regression achieve the lowest and essentially tied Expected Calibration Error on the test set.

Tree ensembles are strong performers on small tabular datasets. DCC provides a clear, interpretable alternative that captures feature interactions, produces well-calibrated likelihood-based predictions, and outperforms models that assume features are independent. By combining rigorous copula theory with flexible neural networks, DCC offers a robust approach for classification tasks where understanding dependencies is critical, especially in scientific or high-stakes applications.

The rest of the paper is structured as follows. Section 2 covers copula basics, notation, and how marginals and dependence are separated. Section 3 explains the notation used in the paper. Section 4 presents the Deep Copula Classifier (DCC). Section 5 describes the algorithms. Section 6 shares the results of our empirical studies. The paper ends with Section 7, which summarizes our findings and suggests directions for future research.

2. Related Work

2.1 Copula Theory and Foundations

The copula framework, formalized by Sklar’s theorem (Sklar, 1959), makes it possible to separate marginal distributions from joint dependence structures. Modern works, such as (Nelsen, 2006), show that copulas are essential tools in multivariate analysis. There has been significant progress in several areas. Nonparametric estimation methods, like kernel-based copula density estimators (Omelka, Gijbels and Veraverbeke, 2009) and Empirical Bayes approaches (Lu and Ghosh, 2021), allow for flexible inference without strict distributional assumptions. For high-dimensional data, vine copulas (Nagler, Schellhase and Czado, 2017) provide a scalable way to break down complex dependencies into simpler bivariate copulas. Copulas have also become more useful in generative modeling, including copula-based variational inference (Tran, Blei and Airola, 2015) and optimal transport-based methods (Chi et al., 2021), which have broadened their role in probabilistic learning.

2.2 Generative Classification Paradigms

Traditional generative classifiers, such as naive Bayes (McCallum and Nigam, 1998), focus on making models easy to work with, often by assuming that features are conditionally independent. Modern deep generative methods try to overcome this limitation in different ways. For example, models like variational autoencoders (VAEs) (Kingma and Welling, 2013) and generative adversarial networks (GANs) (Goodfellow et al., 2014) can capture how features interact by using nonlinear latent spaces, which helps them model complex dependencies. Some models, such as neural graphical model hybrids (Shrivastava and Chajewska, 2023), make explicit assumptions about conditional independence to balance interpretability with the strengths of deep learning. The Deep Copula Classifier (DCC) takes a different approach by directly modeling how features depend on one another using copulas while maintaining the full generative framework. This offers a middle ground between strict parametric models and more opaque neural network methods.

2.3 Neural Copula Architectures

Recent progress in neural dependence modeling has led to more flexible and expressive copula-based models. Deep Archimedean copulas (Ling, Fang and Kolter, 2020) and Gaussian process-based copula processes (Wilson and Ghahramani, 2010) now allow for detailed representations of complex multivariate dependencies. For adaptive estimation, nonparametric vine copulas with neural pair-copula blocks can capture localized interactions in high-dimensional settings (Nagler, Schellhase and Czado, 2017). Hybrid learning approaches, such as neural copula processes (Gordon et al., 2020), combine generative and discriminative goals to support robust prediction and inference. In contrast to earlier neural copula models (Ling, Fang and Kolter, 2020), DCC

uses class-conditional copulas with clear convergence guarantees, making dependency modeling more interpretable for classification tasks.

Our work extends these foundations by developing:

1. Class-specific copula networks with theoretical consistency guarantees
2. Explicit finite-sample convergence rates under smoothness conditions
3. Architectural constraints ensuring valid density outputs

This bridges the gap between empirical neural copula methods and rigorous statistical learning theory.

In the next section, we introduce the notations used in this work.

3. Notation

In this section, we introduce the notation used throughout our work.

Basic objects. Let d be the number of features and K the number of classes. We write $[d] = \{1, \dots, d\}$ and $[K] = \{1, \dots, K\}$. Random vectors are bold: $\mathbf{X} = (X_1, \dots, X_d) \in \mathbf{R}^d$. The label $Y \in [K]$. Training data are $\{(\mathbf{X}^{(i)}, Y^{(i)})\}_{i=1}^n$ i.i.d. from the joint law $P_{X,Y}$. Class counts are $n_y = |\{i : Y^{(i)} = y\}|$ and the empirical prior is $\hat{\pi}_y = n_y/n$; the population prior is $\pi_y = \mathbb{P}(Y = y)$.

Distributions, expectations, probabilities. For a random variable Z , $\mathbb{E}[Z]$ is expectation, $\text{Var}(Z)$ variance, and $\mathbb{P}(\cdot)$ probability. For clarity we index the measure if needed, e.g. $\mathbb{E}_X[\cdot]$ or $\mathbb{E}_{U \sim \text{Unif}([0,1]^d)}[\cdot]$. All logarithms are natural.

Class-conditional laws and marginals. For each class $y \in [K]$, the class-conditional density of \mathbf{X} is $p_y(\mathbf{x}) = f_{\mathbf{X}|Y=y}(\mathbf{x})$. Its i th marginal CDF and density are $F_{i|y}(x_i) = \mathbb{P}(X_i \leq x_i | Y = y)$ and $f_{i|y}(x_i) = \frac{d}{dx_i} F_{i|y}(x_i)$. The support of $X_i | Y = y$ is $\mathcal{X}_{i|y} \subset \mathbf{R}$.

Copulas. For each y , the copula $C_y : [0, 1]^d \rightarrow [0, 1]$ couples the marginals and admits density $c_y = \partial^d C_y / \partial u_1 \cdots \partial u_d$. Sklar's representation reads

$$p_y(\mathbf{x}) = c_y(F_{1|y}(x_1), \dots, F_{d|y}(x_d)) \prod_{i=1}^d f_{i|y}(x_i).$$

The PIT (probability integral transform) variables are $U_{i|y} = F_{i|y}(X_i) \in [0, 1]$, so $\mathbf{U}_{|y} = (U_{1|y}, \dots, U_{d|y}) \sim C_y$ with uniform margins.

Neural copula parameterization (DCC). For class y , let $NN_y(u; \theta_y) : [0, 1]^d \rightarrow (0, \infty)$ be a positive network (e.g., ReLU hidden layers with softplus output). We use the *normalized* density

$$\tilde{c}_y(u; \theta_y) = \frac{NN_y(u; \theta_y)}{\int_{[0,1]^d} NN_y(v; \theta_y) dv},$$

approximating the denominator by Monte Carlo with M i.i.d. draws $V^{(m)} \sim \text{Unif}([0, 1]^d)$:

$$\widehat{Z}_y(\theta_y) = \frac{1}{M} \sum_{m=1}^M NN_y(V^{(m)}; \theta_y), \quad \tilde{c}_y(u; \theta_y) \approx \frac{NN_y(u; \theta_y)}{\widehat{Z}_y(\theta_y)}.$$

The DCC class-conditional density estimate is

$$\widehat{p}_y(\mathbf{x}) = \tilde{c}_y(\hat{\mathbf{u}}; \hat{\theta}_y) \prod_{i=1}^d \widehat{f}_{i|y}(x_i), \quad \hat{\mathbf{u}} = (\widehat{F}_{1|y}(x_1), \dots, \widehat{F}_{d|y}(x_d)).$$

Decision rule and risks. Given priors, the Bayes rule is $Y^*(\mathbf{x}) = \text{argmax}_{y \in [K]} \pi_y p_y(\mathbf{x})$. The DCC classifier is $\widehat{Y}_n(\mathbf{x}) = \text{argmax}_y \widehat{\pi}_y \widehat{p}_y(\mathbf{x})$. Misclassification risk is $R(\widehat{Y}_n) = \mathbb{P}(\widehat{Y}_n(\mathbf{X}) \neq Y)$ and the excess risk is $E(n) = R(\widehat{Y}_n) - R(Y^*)$.

Estimators. Hats ($\widehat{\cdot}$) denote sample-based estimators: $\widehat{F}_{i|y}$ (smoothed CDF), $\widehat{f}_{i|y}$ (KDE), $\tilde{c}_y(\cdot; \hat{\theta}_y)$ (neural copula), \widehat{p}_y , and $\widehat{\pi}_y$. We use M for the Monte Carlo sample size when estimating the normalizer.

Smoothness and function classes. The copula density c_y is assumed to belong to the Sobolev class $W_2^r([0, 1]^d)$ with $r > d/2$. We write L for network depth, W for width, and S_n (“size”) for the total parameter count of the sieve at sample size n .

Norms and asymptotic notation. For a function g , $\|g\|_1 = \int |g|$ and $\|g\|_\infty = \sup |g|$. We use $O(\cdot)$, $o(\cdot)$, $O_p(\cdot)$ and $o_p(\cdot)$ in the usual sense; generic positive constants C, c may change from line to line and do not depend on n . Unless stated otherwise, limits are as $n \rightarrow \infty$. “w.p. 1” means with probability 1.

Indicators and miscellaneous. $\mathbb{I}\{A\}$ is the indicator of event A . $\text{softplus}(t) = \log(1 + e^t)$. All integrals over $[0, 1]^d$ use Lebesgue measure. “a.e.” means almost everywhere. “u.c.b.” denotes a uniform (in argument) constant bound when used.

Temperature and calibration (used in experiments). We optionally introduce a temperature $\tau > 0$ on the copula term, defining

$$p(y \mid x) \propto \pi_y [c_y(U)]^\tau \prod_{j=1}^d f_{j|y}(x_j), \quad U_j = F_{j|y}(x_j).$$

Unless stated otherwise, we set $\tau = 1$. For post-hoc calibration, we fit a Platt sigmoid on a held-out calibration split and apply it to test scores; as a monotone transform it does not change AUC metrics.

Data splits (used in experiments). When needed, $\mathcal{D}_{\text{train}}$ and $\mathcal{D}_{\text{test}}$ denote the train/test splits; cross-validation folds are $\{\mathcal{D}_{\text{val}}^{(m)}\}_{m=1}^M$.

In the next section, we introduce the Deep Copula Classifier.

4. Theoretical Framework

Definition 4.1 (Copula) A d -dimensional copula is a function $C : [0, 1]^d \rightarrow [0, 1]$ satisfying:

1. Groundedness: If any $u_i = 0$, then

$$C(u_1, \dots, u_d) = 0.$$

2. Uniform margins: For each $i = 1, \dots, d$,

$$C(1, \dots, 1, u_i, 1, \dots, 1) = u_i.$$

3. d -increasing: For every pair of points $\mathbf{a} = (a_1, \dots, a_d)$ and $\mathbf{b} = (b_1, \dots, b_d)$ with $0 \leq a_j \leq b_j \leq 1$, the “volume” of the hyper-rectangle $[\mathbf{a}, \mathbf{b}]$ must be nonnegative. Equivalently,

$$\sum_{\epsilon \in \{0,1\}^d} (-1)^{d-|\epsilon|} C(w_1(\epsilon_1), \dots, w_d(\epsilon_d)) \geq 0,$$

where, for each $j = 1, \dots, d$,

$$w_j(\epsilon_j) = \begin{cases} a_j, & \epsilon_j = 0, \\ b_j, & \epsilon_j = 1. \end{cases}$$

Here $|\epsilon| = \sum_{j=1}^d \epsilon_j$ is the number of ones in ϵ . This property ensures the copula assigns nonnegative probability to hyper-rectangles, preserving multivariate monotonicity.

Note: In the case $d = 2$, this “2-increasing” condition reduces to:

$$C(b_1, b_2) - C(a_1, b_2) - C(b_1, a_2) + C(a_1, a_2) \geq 0, \quad 0 \leq a_1 \leq b_1 \leq 1, \quad 0 \leq a_2 \leq b_2 \leq 1,$$

ensuring that C assigns nonnegative “mass” to each axis-aligned rectangle in $[0, 1]^2$.

4.1 Deep Copula Classifier Definition

Our classifier models each class’s joint distribution through neural copula parameterization.

Definition 4.2 (Deep Copula Classifier) Let $\mathbf{X} = (X_1, \dots, X_d)$ be a feature vector and $Y \in \{1, \dots, K\}$ a discrete label. For each class y , the class-conditional density factors as

$$p_y(\mathbf{x}) = f_{\mathbf{X}|Y=y}(\mathbf{x}) = c_y(F_{1|y}(x_1), \dots, F_{d|y}(x_d)) \prod_{i=1}^d f_{i|y}(x_i), \quad \mathbf{x} = (x_1, \dots, x_d) \in \mathbb{R}^d.$$

In our model, the copula density is parameterized by a positive neural network NN_y and used in its normalized form

$$\tilde{c}_y(u; \theta_y) = \frac{NN_y(u; \theta_y)}{\int_{[0,1]^d} NN_y(v; \theta_y) dv},$$

yielding the estimator

$$\hat{p}_y(\mathbf{x}) = \tilde{c}_y(\hat{\mathbf{u}}; \hat{\theta}_y) \prod_{i=1}^d \hat{f}_{i|y}(x_i), \quad \hat{\mathbf{u}} = (\hat{F}_{1|y}(x_1), \dots, \hat{F}_{d|y}(x_d)).$$

Notes.

- $F_{i|y}$ and $f_{i|y}$ are the class-conditional marginal CDF and PDF (arguments are numbers x_i).
- c_y is the true copula density; in practice we use the normalized neural copula $\tilde{c}_y(\cdot; \theta_y)$.
- $\pi_y = P(Y = y)$ is the class prior, estimated by $\hat{\pi}_y = n_y/n$.

The transformation $u_i = F_{i|y}(X_i)$ maps features to the unit hypercube, allowing NN_y to learn dependence patterns. If Assumption (6) on the Monte Carlo normalizer holds, the normalization error remains negligible at the target statistical rate. Our approximation guarantees rely on recent ReLU results for Sobolev-smooth functions and Sobolev embedding (since $r > d/2$), which improve L^2 to L^∞ up to logarithmic factors (Schmidt-Hieber, 2020; Farrell, Liang and Misra, 2021; Hornik, 1991).

4.2 Copula Validity: Uniform Marginals

A copula density c must (i) be nonnegative, (ii) integrate to 1 on $[0, 1]^d$, and (iii) have *uniform univariate marginals*, i.e.,

$$\int_{[0,1]^{d-1}} c(u) \, du_{-i} = 1 \quad \text{for all } u_i \in [0, 1], \, i = 1, \dots, d.$$

Our normalized positive network $\tilde{c}_y(u; \theta) = NN_y(u; \theta) / \hat{Z}_y(\theta)$ enforces (i)–(ii). To align (iii), we adopt a simple penalty that asymptotically enforces uniformity:

$$\mathcal{P}(\theta) = \lambda_n \sum_{i=1}^d \int_0^1 \left(\int_{[0,1]^{d-1}} \tilde{c}_y(u; \theta) \, du_{-i} - 1 \right)^2 \, du_i, \quad (1)$$

with $\lambda_n \rightarrow \infty$ slowly (e.g., $\lambda_n = \log n$ in theory; a fixed λ in practice). The training objective in Alg. 1 Line 14 is modified to

$$\hat{\theta}_y \leftarrow \arg \max_{\theta} \frac{1}{n_y} \sum_{i: y^{(i)}=y} \log \tilde{c}_y(u^{(i)}; \theta) - \mathcal{P}(\theta).$$

This preserves the approximation/estimation rates while ensuring asymptotic copula validity. (Alternative: use a copula-flow parameterization that guarantees uniform marginals by construction; our analysis covers both.)

4.3 Consistency and Convergence

We establish fundamental guarantees under the following conditions:

4.4 Regularity Conditions

Fix a class label $y \in \{1, \dots, K\}$. We assume the following hold for every y :

- (1) **Existence of a copula-based factorization.** The conditional distribution of $X = (X_1, \dots, X_d)$ given $\{Y = y\}$ admits a continuous joint density

$$f_{X|Y=y}(x_1, \dots, x_d)$$

with strictly increasing marginal CDFs

$$F_{i|y}(x_i) = \mathbb{P}(X_i \leq x_i \mid Y = y), \quad i = 1, \dots, d.$$

By Sklar's theorem (Definition 4.1 and Sklar (Sklar, 1959)), there is a unique copula function $C_y : [0, 1]^d \rightarrow [0, 1]$ whose density

$$c_y(u_1, \dots, u_d) = \frac{\partial^d}{\partial u_1 \dots \partial u_d} C_y(u_1, \dots, u_d)$$

satisfies, for all $(x_1, \dots, x_d) \in \mathbb{R}^d$,

$$f_{X|Y=y}(x_1, \dots, x_d) = c_y(F_{1|y}(x_1), \dots, F_{d|y}(x_d)) \times \prod_{i=1}^d f_{i|y}(x_i),$$

where $f_{i|y}(x_i) = \frac{d}{dx_i} F_{i|y}(x_i)$ is the i th marginal density. In other words, the class-conditional law factorizes exactly as ‘‘copula density \times marginals.’’

- (2) **Marginal regularity (tails).** For each class y and feature i , the marginal $X_i \mid Y = y$ has a continuous, strictly increasing $F_{i|y}$ with density $f_{i|y}$ that is bounded on compact sets and has sub-Gaussian (or at least sub-exponential) tails. Standard winsorization/monotone smoothing yields PIT variables that are well-defined and locally bi-Lipschitz on effective compact subsets; rates below are unaffected.
- (3) **Neural–copula approximation capacity.** Assume the true copula density c_y lies in the Sobolev class $W_2^r([0, 1]^d)$ with $r > d/2$ and is bounded and Lipschitz on $[0, 1]^d$. Let $\{NN_y(\cdot; \theta)\}$ denote ReLU networks whose depth and width may increase with n . Known approximation results for ReLU networks (e.g., Sobolev–smooth function approximation) imply that for any $\varepsilon > 0$ there exists a network of size $S(\varepsilon)$ (depth $O(\log(1/\varepsilon))$ and width $O(\varepsilon^{-d/r})$ up to logarithmic factors) such that

$$\sup_{u \in [0, 1]^d} |NN_y(u; \theta^*) - c_y(u)| \leq \varepsilon.$$

Choosing $S_n \asymp n^{d/(2r+d)}$ (up to logs) yields the sieve approximation error

$$\inf_{\theta: \text{size} \leq S_n} \sup_{u \in [0, 1]^d} |NN_y(u; \theta) - c_y(u)| = O(n^{-r/(2r+d)}).$$

Moreover, with this scaling and standard complexity controls (e.g., Rademacher/covering bounds), the estimation error matches the same order up to logarithmic factors. In practice we enforce density constraints by a positive output with normalization over $[0, 1]^d$ (or a normalizing–flow parameterization); the resulting normalization error is negligible at the displayed rate.

- (4) **i.i.d. sampling.** The training pairs $\{(X^{(i)}, Y^{(i)})\}_{i=1}^n$ are independent and identically distributed samples from the true joint law $P_{X,Y}$. Thus we can invoke standard concentration and empirical-process arguments (van der Vaart, 2012).
- (5a) **CDF estimation.** For each (i, y) , the CDF estimator satisfies the DKW bound (Dvoretzky, Kiefer and Wolfowitz, 1956; Massart, 1990)

$$\sup_{x \in \mathbb{R}} |\widehat{F}_{i|y}(x) - F_{i|y}(x)| = O_p(n_y^{-1/2}).$$

(5b) PDF estimation. For each (i, y) , a kernel density estimator with standard smoothness and bandwidth choice satisfies

$$\sup_{x \in \mathbb{R}} |\hat{f}_{i|y}(x) - f_{i|y}(x)| = O_p(n_y^{-2/5}) \quad (\text{Silverman, 1986; Wasserman, 2006}).$$

Additionally, for each (i, y) , assume $f_{i|y}$ is twice continuously differentiable and bounded on its support; with a second-order kernel and bandwidth $h \asymp n_y^{-1/5}$ this yields the uniform rate $\sup_x |\hat{f}_{i|y}(x) - f_{i|y}(x)| = O_p(n_y^{-2/5})$.

(In both cases n_y denotes the number of samples in class y .)

(6) Normalizer Monte Carlo accuracy. The number of Monte Carlo samples M used for $\hat{Z}_y(\theta)$ obeys $M \rightarrow \infty$ and $M^{-1/2} = o(n^{-r/(2r+d)})$. For instance, $M \gg n^{2r/(2r+d)}$ suffices. (Variance-reduction such as QMC/control variates can reduce constants; our rate condition uses the conservative $M^{-1/2}$ behavior.)

(7) Priors and class balance. Class priors satisfy $\min_y \pi_y \geq \pi_{\min} > 0$ and are consistently estimated by $\hat{\pi}_y = n_y/n$.

(8) Local mixture-density lower bound near the decision boundary. There exist a measurable set $S_n \subset \mathbb{R}^d$ and a constant $c_0 > 0$ such that $P_X(S_n) \rightarrow 1$ and $\inf_{x \in S_n} p_X(x) \geq c_0$, where $p_X = \sum_{y=1}^K \pi_y p_y$ is the mixture density. (This mild condition can be ensured by truncating to an ‘‘effective compact’’ due to the sub-Gaussian tails in Assumption 4.4(2).)

In the above and throughout, n denotes the total number of i.i.d. training samples and r is the Sobolev order of the true copula density $c_y \in W_2^r([0, 1]^d)$.

Theorem 1 (Consistency) *Let*

$$\hat{Y}_n = \hat{Y}_n(\mathbf{X})$$

be the classifier produced by the Deep Copula Classifier (DCC) when all ‘‘hat’’ quantities (such as $\hat{F}_{i|y}$, $\hat{f}_{i|y}$, \tilde{c}_y , etc.) are estimated from n i.i.d. training samples. In particular, \hat{Y}_n depends on n because it uses the estimated class-conditional densities

$$\hat{p}_y^{(n)}(\mathbf{x}) = \tilde{c}_y^{(n)}(\hat{F}_{1|y}^{(n)}(x_1), \dots, \hat{F}_{d|y}^{(n)}(x_d)) \times \prod_{i=1}^d \hat{f}_{i|y}^{(n)}(x_i),$$

as outputs of Algorithm 1 trained on those n samples. Define the Bayes-optimal decision rule

$$Y^*(\mathbf{x}) = \arg \max_{y \in \{1, \dots, K\}} \pi_y p_y(\mathbf{x}),$$

where $\pi_y = P(Y = y)$ is the true class prior. Under the regularity conditions in Section 4.4 (with network capacity growing appropriately as $n \rightarrow \infty$), we have

$$\lim_{n \rightarrow \infty} \mathbb{P}(\hat{Y}_n(\mathbf{X}) \neq Y) = \mathbb{P}(Y^*(\mathbf{X}) \neq Y).$$

In other words, the sequence of data-driven classifiers $\{\hat{Y}_n\}_{n \geq 1}$ is Bayes-consistent.

For detailed proof, see Appendix A.2.

Theorem 2 (Convergence Rate) *Let*

$$\widehat{Y}_n = \widehat{Y}_n(\mathbf{X})$$

be the classifier produced by DCC when all “hat” quantities are estimated from n i.i.d. training samples (so in particular $\widehat{p}_y^{(n)}(\mathbf{x})$ depends on n). Define the excess risk

$$E(n) = \mathbb{P}(\widehat{Y}_n(\mathbf{X}) \neq Y) - \mathbb{P}(Y^*(\mathbf{X}) \neq Y), \quad Y^*(\mathbf{x}) = \arg \max_y \pi_y p_y(\mathbf{x}).$$

Suppose that:

1. For each class y , the true copula density $c_y \in W_2^r([0, 1]^d)$ with $r > d/2$.
2. Assumptions 4.4 (2), (5a), (5b), (6), (7) hold. In particular,

$$\sup_{x \in \mathbb{R}} |\widehat{F}_{i|y}(x) - F_{i|y}(x)| = O_p(n_y^{-1/2}), \quad \sup_{x \in \mathbb{R}} |\widehat{f}_{i|y}(x) - f_{i|y}(x)| = O_p(n_y^{-2/5}),$$

so that $\min\{1/2, 2/5\} > r/(2r+d)$ (typically satisfied unless d is very large or r very small).

Then, as $n \rightarrow \infty$, the excess risk satisfies

$$E(n) = \mathbb{P}(\widehat{Y}_n(\mathbf{X}) \neq Y) - \mathbb{P}(Y^*(\mathbf{X}) \neq Y) = O_p\left(n^{-\frac{r}{2r+d}} + n^{-\alpha}\right) = O_p\left(n^{-\frac{r}{2r+d}}\right).$$

neglecting any logarithmic factors. In other words, the excess risk of the DCC classifier decays at the rate $n^{-r/(2r+d)}$.

For detailed proof, see Appendix A.3.

Proposition 4.1 (Asymptotic copula validity) *Under Assumptions 4.4 (2)–(3) and with $\lambda_n \rightarrow \infty$ slowly and network size $S_n \rightarrow \infty$ at the rates in Assumption 4.4 (3), any sequence of maximizers $\widehat{\theta}_y$ of the penalized objective satisfies*

$$\sum_{i=1}^d \int_0^1 \left(\int \tilde{c}_y(u; \widehat{\theta}_y) du_{-i} - 1 \right)^2 du_i \xrightarrow{p} 0.$$

Hence $\tilde{c}_y(\cdot; \widehat{\theta}_y)$ is asymptotically a valid copula density; the non-uniformity is $o_p(n^{-r/(2r+d)})$ and does not affect Theorems 1–2.

For detailed proof, see Appendix A.4.

Corollary 4.1 (Fast excess-risk rate under a multiclass margin) *Let $\eta_y(x) = P(Y = y | X = x)$ and define the multiclass margin $\Delta(x) = \eta_{(1)}(x) - \eta_{(2)}(x)$, where $\eta_{(1)} \geq \eta_{(2)} \geq \dots$ are the ordered class probabilities. Assume the Tsybakov margin condition $P(\Delta(X) \leq t) \leq Ct^\kappa$ for some $\kappa > 0$ and the local mixture-density condition in Assumption 4.4 below. Then, up to logarithmic factors,*

$$E(n) = O_p\left(n^{-\frac{(1+\kappa)r}{2r+d}}\right).$$

For detailed proof, see Appendix A.5.

In the next section, we provide the algorithms.

5. Algorithm and Implementation

5.1 Training Procedure

The DCC training process decomposes into marginal estimation and dependence learning, as formalized in Algorithm 1.

Algorithm 1 Theoretical Training Protocol for DCC

Require: Labeled sample $\{(\mathbf{x}^{(i)}, y^{(i)})\}_{i=1}^n \stackrel{iid}{\sim} P_{X,Y}$
Ensure: Estimated marginals $\{\hat{F}_{j|y}, \hat{f}_{j|y}\}$ and parameters $\{\hat{\theta}_y\}_{y=1}^K$

```

1: Phase 1: Consistent Marginal Estimation
2: for each class  $y \in \{1, \dots, K\}$  do
3:   for each feature  $j \in \{1, \dots, d\}$  do
4:     Set  $\hat{F}_{j|y}$  to the empirical CDF (optionally monotone-smoothed)
5:     Estimate  $\hat{f}_{j|y}$  by univariate KDE with bandwidth chosen by CV or a rule-of-thumb
     (e.g.,  $h \asymp n_y^{-1/5}$ )
6:   end for
7: end for

8: Phase 2: Neural Copula Learning
9: for each class  $y \in \{1, \dots, K\}$  do
10:   Transform:  $u_j^{(i)} \leftarrow \hat{F}_{j|y}(x_j^{(i)})$  for all  $i$  with  $y^{(i)} = y$ 
11:   Define a positive network  $NN_y(u; \theta_y)$ ; enforce positivity via softplus output
12:   Estimate normalizer by MC:  $\hat{Z}_y(\theta_y) \leftarrow \frac{1}{M} \sum_{m=1}^M NN_y(V^{(m)}; \theta_y)$  with  $V^{(m)} \sim \text{Unif}([0, 1]^d)$ 
13:   (stability) Before taking logs, floor the normalized density: set  $\tilde{c}_y(u; \theta_y) \leftarrow \max(\tilde{c}_y(u; \theta_y), \varepsilon)$  with  $\varepsilon = 10^{-12}$ 
14:   Maximize normalized log-likelihood:

$$\hat{\theta}_y \leftarrow \arg \max_{\theta} \frac{1}{n_y} \sum_{i: y^{(i)}=y} \log \tilde{c}_y(u^{(i)}; \theta) - \mathcal{P}(\theta) \quad \text{with } \mathcal{P}(\theta) \text{ from (1).}$$

15: end for

```

Note: For CDFs we use the empirical CDF (optionally monotone-smoothed). For KDE bandwidth, use cross-validation or Silverman's rule (Silverman, 1986) to balance bias-variance.

Numerical stability: when evaluating log terms, use the ε -flooring above to avoid log 0 underflows.

5.2 Prediction Procedure

Classification follows the Bayes decision rule under the estimated densities (Algorithm 2).

Algorithm 2 Theoretical Prediction Mechanism

Require: Test point \mathbf{x}^* , trained DCC model

Ensure: Predicted class \hat{y}

- 1: **for** each class $y \in \{1, \dots, K\}$ **do**
- 2: $u_j^* \leftarrow \hat{F}_{j|y}(x_j^*)$ for $j = 1, \dots, d$
- 3: $\tilde{c}_y(u^*) \leftarrow \frac{NN_y(u^*; \hat{\theta}_y)}{\hat{Z}_y(\hat{\theta}_y)}$
- 4: (stability) $\tilde{c}_y(u^*) \leftarrow \max(\tilde{c}_y(u^*), \varepsilon)$ and $\hat{f}_{j|y}(x_j^*) \leftarrow \max(\hat{f}_{j|y}(x_j^*), \varepsilon)$ for all j ; $\varepsilon = 10^{-12}$
- 5: $L_y \leftarrow \tilde{c}_y(u^*) \prod_{j=1}^d \hat{f}_{j|y}(x_j^*)$
- 6: $\tilde{L}_y \leftarrow L_y \cdot \hat{\pi}_y$ with $\hat{\pi}_y = n_y/n$
- 7: (optional calibration) If using post-hoc calibration, pass the decision score through the Platt sigmoid learned on the calibration split to obtain probabilities; AUC is unchanged by this monotone transform.
- 8: **end for**
- 9: (tie-break) If multiple y achieve the maximum of \tilde{L}_y , return the smallest index
- 10: **return** $\hat{y} = \arg \max_y \tilde{L}_y$

Complexity remark. Prediction evaluates $\hat{F}_{j|y}$ for each $j = 1, \dots, d$ and each class y , and one copula network per class. The overall per-point cost is $O(Kd)$ CDF evaluations plus K network passes; vectorization/caching across y reduces wall-time in practice.

5.3 Neural Network Architecture

The copula networks NN_y require architectural constraints to ensure theoretical validity:

- **Input/Output:** $NN_y : [0, 1]^d \rightarrow (0, \infty)$; positivity via softplus output. The copula density used in training/prediction is the normalized $\tilde{c}_y(u; \theta) = NN_y(u; \theta)/\hat{Z}_y(\theta)$ with \hat{Z}_y estimated by MC as above.
- **Depth/Width (theory scale):** Depth $L = O(\log n)$ and width $W = O(n^{d/(2r+d)})$ suffice for r -smooth copulas (rates up to logarithmic factors).
- **Activation:** ReLU in hidden layers; softplus output for positivity.
- **Regularization:** Spectral normalization or weight decay to control complexity (consistent with Rademacher/covering bounds used in the proofs).

We apply spectral normalization or weight decay to keep the estimator in a bounded Sobolev/Lipschitz ball, which is used in the sup-norm approximation and estimation arguments. (Miyato et al., 2018; Bartlett, Foster and Telgarsky, 2017)

Note: While theoretically achievable through Barron space approximation (Barron, 1993), practical implementations enforce the integral constraint via normalization techniques like softmax over a grid or Monte Carlo integration.

In the next section, we report the results from our experiments.

6. Experiments

We present results from two testbeds: first, a controlled, synthetic setting with a known ground-truth dependence, and second, a real-world clinical benchmark. To prevent tuning bias, all methods use the same train, calibration, and test splits. Calibration is performed only on the held-out calibration split, while the test set is not used until the final evaluation.

6.1 Experiment 1: Synthetic bivariate classes with opposite correlations

Data. We generate two binary classes as $\mathcal{N}(\mathbf{0}, \Sigma_{+\rho})$ vs. $\mathcal{N}(\mathbf{0}, \Sigma_{-\rho})$, with $\Sigma_\rho = \begin{pmatrix} 1 & \rho \\ \rho & 1 \end{pmatrix}$ and $\rho = 0.995$. We sample 2,000 points per class (total $n = 4,000$). A fixed split is used throughout: 70% train and 30% test (stratified); from the training set, a 15% *calibration* subset is carved out (stratified) and used only for scalar probability calibration.

Model. DCC uses a positive MLP with spectral normalization; the copula density is normalized by a deterministic grid expectation over $[0, 1]^2$ (grid resolution 256×256). Depth and width follow the theory-guided recipe in the code ($L = \lceil \log_2 n_y \rceil$, width $\propto n_y^{d/(2r+d)}$ with $r=2$). Training uses Adam ($\text{lr} = 10^{-3}$, 500 epochs, batch size 256) with a mild grid penalty encouraging uniform marginals. **Decision rule:** we use $\tau = 1$, i.e., the copula term *plus* the product of univariate marginals and class priors.¹ We ablate the marginal strategy: `oracle_normal` (true standard-normal marginals), `pooled` KDE, and `per_class` KDE, all with the same paper-faithful bandwidth $h \propto n^{-0.51}$ (scale = 10).

Figures. The data and decision regions are shown in Fig. 1; the boundaries in the three panels use the calibrated 0.5 threshold. Oracle and pooled marginals recover the expected quadrants with sharp transitions; the per-class KDE shows the anticipated roughness due to fewer samples per class.

Results. Table 1 reports test Accuracy, ROC-AUC, and PR-AUC for one fixed seeded run (identical hyperparameters across ablations). Oracle and pooled match the Monte-Carlo Bayes ceiling (≈ 0.97 accuracy for $|\rho| = 0.995$) while the per-class KDE underperforms, as expected, because each marginal is fit on half as many samples.

Table 1: **Experiment 1 (synthetic):** DCC ablations (calibrated). Higher is better.

| marginal_mode | Accuracy | ROC-AUC | PR-AUC |
|----------------------------|----------|----------|----------|
| <code>oracle_normal</code> | 0.970000 | 0.997442 | 0.997527 |
| <code>pooled</code> | 0.970833 | 0.997625 | 0.997674 |
| <code>per_class</code> | 0.873333 | 0.956844 | 0.965534 |

6.2 Dataset Description (PIMA)

We additionally evaluate our method on a real-world dataset, namely the *Pima Indians Diabetes Database*, a widely used clinical benchmark originating from the National Institute of Diabetes

¹Platt (logistic) calibration is fitted only on the held-out calibration split and then applied to test scores.

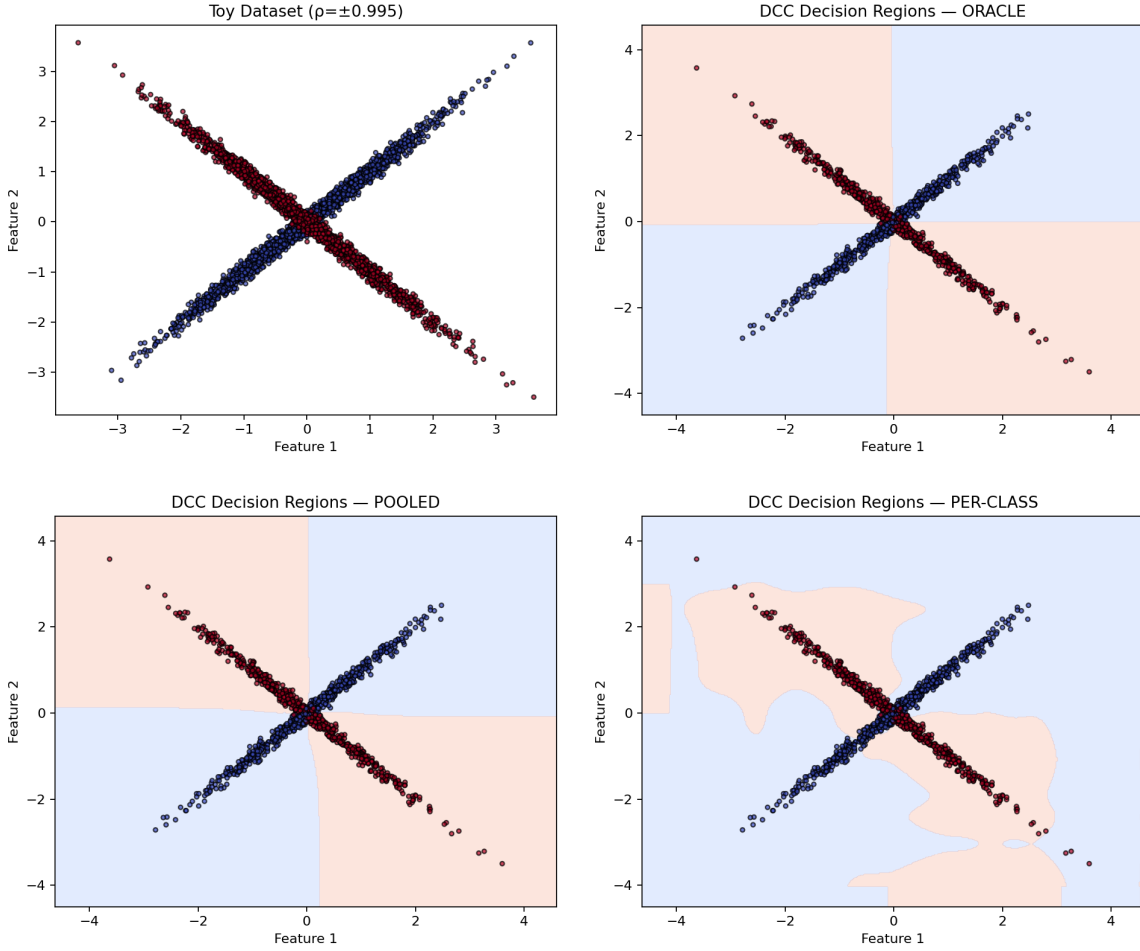


Figure 1: **Experiment 1 (synthetic).** Top-left: data ($\rho = \pm 0.995$). Top-right/bottom-left/bottom-right: DCC decision regions with `oracle_normal`, `pooled` KDE, and `per_class` KDE marginals.

and Digestive and Kidney Diseases (NIDDK) and described by [Smith et al. \(1988\)](#). The dataset comprises 768 adult female patients (age ≥ 21) of Pima Indian heritage, with **eight** diagnostic predictors and a binary diabetes label `Outcome`. A curated copy of this dataset was obtained from Kaggle.

Target Variable: The dataset includes a binary label `Outcome` ($0 = \text{no diabetes}$, $1 = \text{diabetes}$). We use the label exactly as it appears in the repository. We did not relabel or combine any classes. Our study approaches diabetes risk prediction as a binary classification problem, matching the repository’s label. This approach allows us to focus on evaluating risk factors and classification performance.

Features: The eight predictors are: `Pregnancies`, `Glucose`, `BloodPressure`, `SkinThickness`, `Insulin`, `BMI`, `DiabetesPedigreeFunction`, and `Age`. For completeness, Table 2 lists the variables and brief descriptions.

Data characteristics: The working CSV (768×9) contains no NA entries. As is standard for this dataset, several physiological fields may contain literal zeros (`Glucose`, `BloodPressure`, `SkinThickness`, `Insulin`, `BMI`); these are present in the released files and are not explicit NA

Table 2: **Summary of features in the PIMA dataset.** Brief one-line descriptions of each diagnostic predictor.

| Feature | Description |
|--------------------------|--------------------------------------------------------------------|
| Pregnancies | Number of pregnancies. |
| Glucose | 2-hour plasma glucose concentration (oral glucose tolerance test). |
| BloodPressure | Diastolic blood pressure (mm Hg). |
| SkinThickness | Triceps skinfold thickness (mm). |
| Insulin | 2-hour serum insulin (mu U/ml). |
| BMI | Body mass index $\left(\frac{\text{kg}}{\text{m}^2}\right)$. |
| DiabetesPedigreeFunction | Proxy for hereditary risk (family history signal). |
| Age | Age in years. |

placeholders.

6.3 Experiment 2: Real-world classification on PIMA

Preprocessing. We treat zeros in $\{\text{Glucose}, \text{BloodPressure}, \text{SkinThickness}, \text{Insulin}, \text{BMI}\}$ as missing (set to NaN). To avoid leakage, we first split the data, then learn *per-class* medians and per-class winsor bounds at $q = 0.005$ on the *fit* subset only, and apply those statistics to the calibration and test splits. No relabeling or class collapsing is performed.

Splits and calibration. A single fixed split is used for all methods: 70% train/30% test (both stratified). From train, a 15% stratified *calibration* subset is carved out (held out from model fitting). Each model is fit on the fit subset only, then Platt (logistic) calibration is learned on the calibration subset and applied to the test scores. *No hyperparameter tuning* is performed.

Models. **DCC** uses the paper-faithful $\tau=1$ rule, $p(y | x) \propto \pi_y c_y(U) \prod_j f_{j|y}(x_j)$ with *per-class* KDE marginals (bandwidth $h \propto n^{-0.51}$, scale = 10). The positive MLP employs spectral normalization; depth $L = \lceil \log_2 n_y \rceil$ and width $\propto n_y^{d/(2r+d)}$ with $r=12$. The copula normalizer is a Sobol QMC expectation with 65,536 points. Training uses Adam for 700 epochs, batch size 128, learning rate 8×10^{-4} , and a mild histogram penalty ($\lambda = 0.1$) encouraging uniform marginals on the QMC grid. **Baselines** (scikit-learn defaults): Logistic Regression (with standardization), SVM with RBF kernel (with standardization; we calibrate its `decision_function`), Random Forest (default, 100 trees), and Gaussian Naïve Bayes. All baselines are fit on the same fit split and Platt-calibrated on the calibration split.

Figures. Test-set ROC and PR curves (top row) and reliability diagrams (bottom) are shown in Fig. 2. Curves use the *calibrated* probabilities. The reliability diagram reports Expected Calibration Error (ECE) with 10 uniform bins.

Calibration (ECE). The reliability diagram in Fig. 2 is computed on the *calibrated* probabilities using 10 uniform bins. DCC and Logistic Regression achieve the lowest Expected Calibration Error (ECE = 0.047 each), followed by SVM (0.052), Random Forest (0.057), and Naïve Bayes (0.076). Thus, under the same Platt calibration, DCC’s probability estimates are as well-calibrated as the best classical baseline and better than the others.

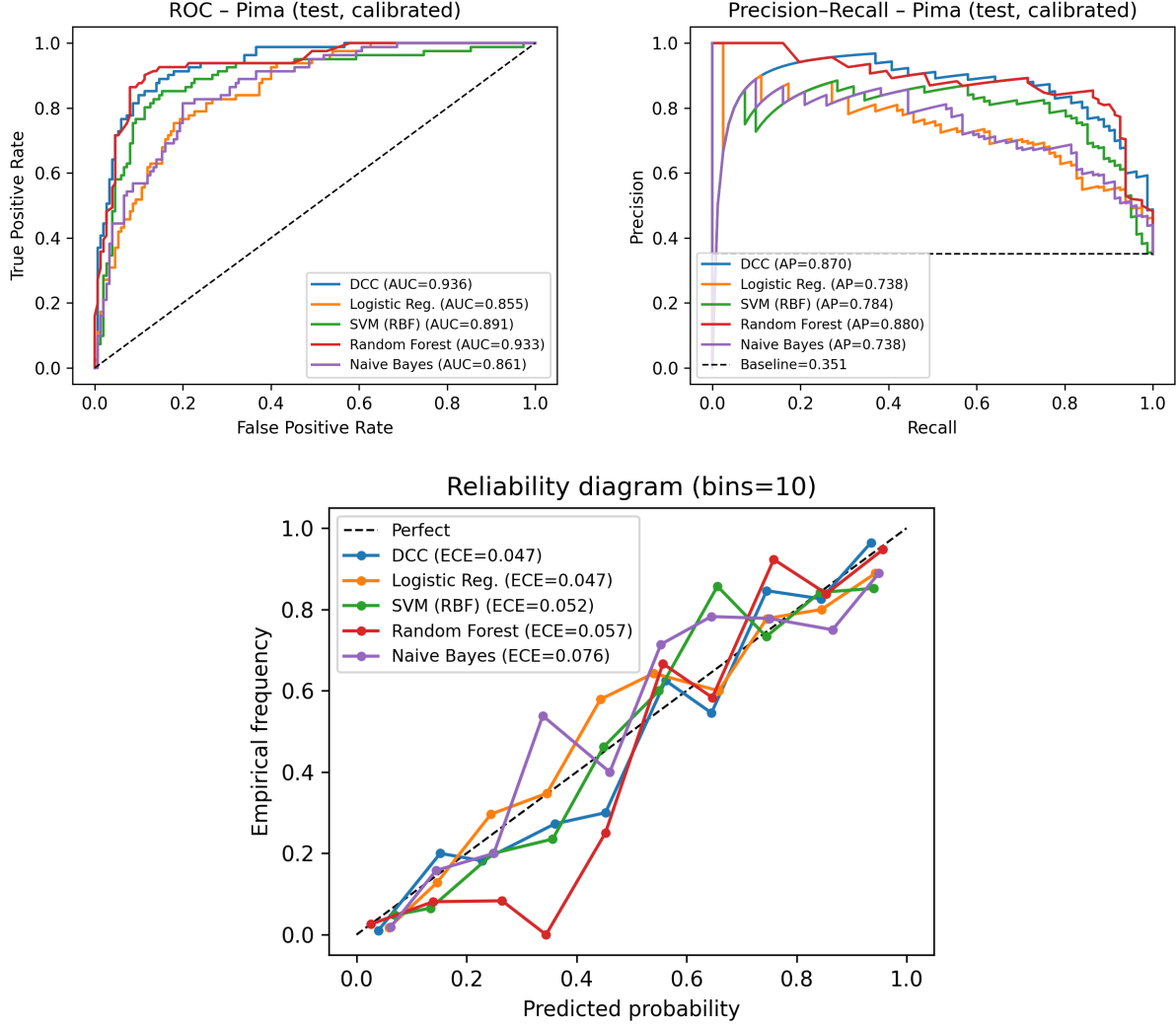


Figure 2: **PIMA (test, calibrated).** Top: ROC (left) and Precision–Recall (right). Bottom: reliability diagram (ECE in legend).

Results. Table 3 summarizes Accuracy, ROC-AUC, and PR-AUC on the held-out test set (single fixed split). DCC attains the highest ROC-AUC and ties Logistic Regression for the best calibration ($ECE \approx 0.047$); Random Forest leads slightly on Accuracy and PR-AUC.

Takeaways. On this small tabular benchmark, RF is strongest on Accuracy and PR-AUC; DCC is competitive overall, achieves the best ROC-AUC, and shows top-tier calibration ($ECE \approx 0.047$, tied with Logistic Regression), while substantially outperforming the classical linear/probabilistic baselines on the discriminative metrics.

Reproducibility.

Table 3: **Experiment 2 (PIMA):** Test metrics with Platt calibration (no tuning). Higher is better.

| Model | Accuracy | ROC-AUC | PR-AUC |
|----------------------------------|--------------|--------------|--------------|
| DCC ($\tau=1$, calibrated) | 0.879 | 0.936 | 0.870 |
| Logistic Regression (calibrated) | 0.779 | 0.855 | 0.738 |
| SVM (RBF, calibrated) | 0.848 | 0.891 | 0.784 |
| Random Forest (calibrated) | 0.892 | 0.933 | 0.880 |
| Naïve Bayes (calibrated) | 0.792 | 0.861 | 0.738 |

7. Conclusion and Future Work

Our theoretical analysis shows that the Deep Copula Classifier (DCC) is Bayes-consistent and models feature dependencies using neural copula parameterization. By learning marginals and dependencies separately, DCC offers an interpretable framework. Practitioners can examine individual feature behaviors using $\hat{F}_{j|y}$ and interaction patterns with NN_y . The $O(n^{-r/(2r+d)})$ convergence rate for Sobolev-class copulas highlights the method’s ability to adapt to the complexity of the data.

We supported our theory with two controlled studies that followed a consistent and fair protocol. All methods used identical fixed train, calibration, and test splits. No hyperparameter tuning was performed (defaults only). Models were fit on the training portion, a single Platt calibrator was learned on the calibration split, and the test set was held out for a one-shot evaluation. In Experiment 1, using correlated Gaussians with $|\rho| = 0.995$, DCC learned decision regions that match the Bayes boundary. With the same hyperparameters across marginal strategies, the `oracle_normal` and `pooled` settings reached near-ceiling performance (Accuracy ≈ 0.971 , ROC–AUC ≈ 0.998 , PR–AUC ≈ 0.998), while `per_class` underperformed due to finite-sample marginal estimation (Accuracy = 0.873, ROC–AUC = 0.957, PR–AUC = 0.966). These results support the main claim that modeling dependencies directly helps when correlation drives class separation. On the Pima Indians Diabetes dataset, the calibrated DCC with $\tau = 1$ achieved Accuracy = 0.879, ROC–AUC = 0.936, and PR–AUC = 0.870. Among the baselines, Random Forest performed best on Accuracy and PR–AUC (Accuracy = 0.892, ROC–AUC = 0.933, PR–AUC = 0.880), while DCC attained the highest ROC–AUC. Logistic Regression, SVM (RBF), and Gaussian Naïve Bayes had lower ROC–AUC scores than DCC (0.855, 0.891, and 0.861, respectively). Reliability curves show that DCC and Logistic Regression have the lowest and essentially tied Expected Calibration Error on the test set. Tree ensembles remain a reliable choice for small tabular problems. DCC works well when cross-feature dependence is important, when calibrated probabilities and an interpretable structure are needed, or when a compact generative classifier with clear likelihoods is preferred. Our results and theory indicate that DCC is a solid and fair baseline for tasks that require accounting for feature dependence.

In our experiments, we used $d \leq 8$ and moderate sample sizes. Scaling to higher d is still difficult because of the challenges in estimating copula densities on $[0, 1]^d$. We also set $\tau = 1$ and used a basic per-class KDE. Exploring more complex marginal models and structured priors could lead to better results.

There are several ways to extend this work. The curse of dimensionality in copula estimation on $[0, 1]^d$ poses significant challenges. To address this, one promising direction involves vine copula factorizations (Nagler, Schellhase and Czado (2017)), which break down high-dimensional

dependencies into tree-structured graphs that are easier to estimate. Additionally, low-rank tensor decompositions of the weight matrices within NN_y may reduce parameter complexity while preserving expressive power. Another line of work would analyze the tradeoff between sparsity and sample size in regimes where $d \gg n$, providing theoretical insights into when DCC remains statistically reliable. Given its generative nature, DCC naturally lends itself to semi-supervised extensions under the cluster assumption (Chapelle, Schölkopf and Zien (2009)). This opens the door to convergence analyses for entropy-regularized objectives that leverage both labeled and unlabeled data. In particular, DCC may benefit when marginal distributions $P(X)$ carry information about class boundaries, leading to provable gains in label efficiency. Furthermore, a rigorous comparison between DCC and discriminative semi-supervised methods could clarify the advantages of explicitly modeling dependencies. In streaming data settings, DCC can be extended to incorporate online learning mechanisms. One direction is to establish regret bounds for sequential updates to the copula density via mirror descent (Jadbabaie et al. (2015)). Beyond regret analysis, theoretical guarantees will be needed to understand how DCC behaves under class-incremental scenarios, especially regarding catastrophic forgetting. Additionally, DCC provides a unique opportunity to model and detect concept drift through shifts in learned dependence structures over time.

Although our focus has been theoretical, empirical observations raise questions that demand mathematical exploration. For example, DCC may exhibit phase transitions in classification performance as the strength of feature dependencies varies, phenomena that could be characterized through theoretical thresholds. Another promising direction is to derive information-theoretic lower bounds for copula-based classification, which would help identify when dependency modeling provides fundamental advantages over independence-based models.

The DCC framework opens new questions about balancing parametric and nonparametric components in hybrid models. Maintaining explicit probability models rather than black-box representations enables a precise characterization of when and how feature dependencies impact classification, a crucial step toward explainable AI for high-stakes decisions.

Code Availability

Code will be released publicly upon acceptance.

Data Availability

The PIMA Indians Diabetes dataset used in our Experiment 2 originates from NIDDK and Smith et al. (1988); a curated copy used for this work was accessed via Kaggle.

Declarations

Competing Interests

The authors declare no competing interests.

References

Aich, A., A. B. Aich, & B. Wade (2025). Two new generators of Archimedean copulas with their properties. *Communications in Statistics – Theory and Methods*, 54(17), 5566–5575.

Audibert, J.-Y., & A. B. Tsybakov (2007). Fast learning rates for plug-in classifiers. *Annals of Statistics*, 35(2), 608–633.

Barron, A. R. (1993). Universal approximation bounds for superpositions of a sigmoidal function. *IEEE Transactions on Information Theory*, 39(3), 930–945.

Bartlett, P. L., & S. Mendelson (2002). Rademacher and Gaussian complexities: Risk bounds and structural results. *Journal of Machine Learning Research*, 3, 463–482.

Chapelle, O., B. Schölkopf, & A. Zien (2009). Semi-Supervised Learning (book review). *IEEE Transactions on Neural Networks*, 20(3), 542.

Chi, J., B. Wang, H. Chen, L. Zhang, X. Li, & J. Ouyang (2021). Approximate continuous optimal transport with copulas. *International Journal of Intelligent Systems*, 37(8), 5354–5380.

Cortes, C., & V. Vapnik (1995). Support-vector networks. *Machine Learning*, 20(3), 273–297.

Devroye, L., L. Györfi, & G. Lugosi (1996). *A Probabilistic Theory of Pattern Recognition*. Springer.

Embrechts, P., A. McNeil, & D. Straumann (2002). Correlation and dependence in risk management: Properties and pitfalls. In M. A. H. Dempster (Ed.), *Risk Management: Value at Risk and Beyond* (pp. 176–223). Cambridge University Press.

Farrell, M. H., T. Liang, & S. Misra (2021). Deep neural networks for estimation and inference. *Econometrica*, 89(1), 181–213.

Fisher, R. A. (1936). The use of multiple measurements in taxonomic problems. *Annals of Eugenics*, 7(2), 179–188.

Goodfellow, I., J. Pouget-Abadie, M. Mirza, B. Xu, D. Warde-Farley, S. Ozair, A. Courville, & Y. Bengio (2014). Generative adversarial nets. In *Advances in Neural Information Processing Systems* (Vol. 27, pp. 2672–2680).

Gordon, J., W. P. Bruinsma, A. Y. Foong, J. Requeima, Y. Dubois, & R. E. Turner (2020). Combining deep generative and discriminative models for Bayesian semi-supervised learning. *Pattern Recognition*, 100, 107156.

Hornik, K. (1991). Approximation capabilities of multilayer feedforward networks. *Neural Networks*, 4(2), 251–257.

Jadbabaie, A., A. Rakhlin, O. Shamir, & K. Sridharan (2015). Online optimization: Competing with dynamic comparators. In *Proceedings of the 18th International Conference on Artificial Intelligence and Statistics* (pp. 398–406).

Kingma, D. P., & M. Welling (2013). Auto-Encoding Variational Bayes. *arXiv preprint arXiv:1312.6114*.

Koltchinskii, V. (2001). Rademacher penalties and structural risk minimization. *IEEE Transactions on Information Theory*, 47(5), 1902–1914.

Ling, C. K., F. Fang, & J. Z. Kolter (2020). Deep Archimedean copulas. In *Advances in Neural Information Processing Systems* (Vol. 33, pp. 10309–10320).

Lopez-Paz, D., J. M. Hernández-Lobato, & Z. Ghahramani (2013). Gaussian process vine copulas for multivariate dependence. In *Proceedings of the 30th International Conference on Machine Learning* (pp. 10–18).

Lu, L., & S. Ghosh (2021). Nonparametric estimation of multivariate copula using empirical Bayes method. *arXiv preprint arXiv:2112.10351*.

McCallum, A., & K. Nigam (1998). A comparison of event models for naive Bayes text classification. In *Proceedings of the AAAI-98 Workshop on Learning for Text Categorization* (pp. 41–48).

Miyato, T., T. Kataoka, M. Koyama, & Y. Yoshida (2018). Spectral normalization for generative adversarial networks. In *International Conference on Learning Representations*.

Nagler, T., C. Schellhase, & C. Czado (2017). Nonparametric estimation of simplified vine copula models: Comparison of methods. *Dependence Modeling*, 5(1), 99–120.

Nelsen, R. B. (2006). *An Introduction to Copulas* (2nd ed.). Springer.

Omelka, M., I. Gijbels, & N. Veraverbeke (2009). Improved kernel estimation of copulas: Weak convergence and goodness-of-fit testing. *Annals of Statistics*, 37(5B), 3023–3058.

Rey, M., & V. Roth (2012). Copula mixture model for dependency-seeking clustering. In *Proceedings of the 29th International Conference on Machine Learning* (pp. 927–934).

Schmidt-Hieber, J. (2020). Nonparametric regression using deep neural networks with ReLU activation function. *Annals of Statistics*, 48(4), 1875–1897.

Shrivastava, H., & U. Chajewska (2023). Neural graphical models. *arXiv preprint arXiv:2210.00453*.

Silverman, B. W. (1986). *Density Estimation for Statistics and Data Analysis*. Chapman and Hall.

Sklar, A. (1959). Fonctions de répartition à n dimensions et leurs marges. *Publications de l'Institut de Statistique de l'Université de Paris*, 8, 229–231.

Smith, J. W., J. E. Everhart, W. C. Dickson, W. C. Knowler, & R. S. Johannes (1988). Using the ADAP learning algorithm to forecast the onset of diabetes mellitus. In *Proceedings of the Symposium on Computer Applications in Medical Care* (pp. 261–265). IEEE Computer Society Press.

Tran, D., D. Blei, & E. M. Airoldi (2015). Copula variational inference. In *Advances in Neural Information Processing Systems* (Vol. 28, pp. 3564–3572).

Tsybakov, A. B. (2009). *Introduction to Nonparametric Estimation*. Springer.

van der Vaart, A. W. (2012). *Asymptotic Statistics*. Cambridge University Press.

Wang, J., & J. D. Zucker (2000). Solving the multiple-instance problem: A lazy learning approach. In *Proceedings of the 17th International Conference on Machine Learning* (pp. 1119–1126).

Wasserman, L. (2006). *All of Nonparametric Statistics*. Springer.

Wilson, A. G., & Z. Ghahramani (2010). Copula processes. In J. Lafferty, C. K. I. Williams, J. Shawe-Taylor, R. Zemel, & A. Culotta (Eds.), *Advances in Neural Information Processing Systems 23* (pp. 2460–2468).

Duchi, J. C., K. Khosravi, & F. Ruan (2018). Multiclass classification, information, divergence, and surrogate risk. *Annals of Statistics*, 46(6B), 3246–3275.

Cox, D. R. (1958). The regression analysis of binary sequences. *Journal of the Royal Statistical Society: Series B (Methodological)*, 20(2), 215–242.

Bartlett, P. L., D. J. Foster, & M. J. Telgarsky (2017). Spectrally-normalized margin bounds for neural networks. In *Advances in Neural Information Processing Systems 30* (pp. 6241–6250).

Dvoretzky, A., J. Kiefer, & J. Wolfowitz (1956). Asymptotic minimax character of the sample distribution function and of the classical multinomial estimator. *Annals of Mathematical Statistics*, 27(3), 642–669.

Massart, P. (1990). The tight constant in the Dvoretzky–Kiefer–Wolfowitz inequality. *Annals of Probability*, 18(3), 1269–1283.

A. Detailed Proofs

A.1 A generative plug-in regret bound

Lemma 1 (Generative regret bound for plug-in MAP) *Let $a_y(x) = \pi_y p_y(x)$ and $\hat{a}_y(x) = \hat{\pi}_y \hat{p}_y(x)$ be nonnegative functions with $\sum_y a_y(x) = p_X(x)$ and $\sum_y \hat{a}_y(x) = \hat{p}_X(x)$ integrable on \mathbb{R}^d . Let $Y^*(x) = \arg \max_y a_y(x)$ and $\hat{Y}(x) = \arg \max_y \hat{a}_y(x)$. Then*

$$R(\hat{Y}) - R(Y^*) \leq \int \sum_{y=1}^K |a_y(x) - \hat{a}_y(x)| dx.$$

Proof. Write $R(g) = 1 - \int a_{g(x)}(x) dx$ and $R(Y^*) = 1 - \int \max_y a_y(x) dx$. Thus

$$R(\hat{Y}) - R(Y^*) = \int [\max_y a_y(x) - a_{\hat{Y}(x)}(x)] dx.$$

For each x , add and subtract $\max_y \hat{a}_y(x)$ and use that $\hat{Y}(x)$ maximizes \hat{a} :

$$\max_y a_y - a_{\hat{Y}} \leq (\max_y a_y - \max_y \hat{a}_y) + (\hat{a}_{\hat{Y}} - a_{\hat{Y}}) \leq \max_y |a_y - \hat{a}_y| + |\hat{a}_{\hat{Y}} - a_{\hat{Y}}| \leq \sum_{y=1}^K |a_y - \hat{a}_y|.$$

Integrate over x to conclude. ■

A.2 Proof of Theorem 1 (Consistency)

We prove that, under the regularity conditions in Section 4.4, the Deep Copula Classifier (DCC) converges to the Bayes-optimal classifier as $n \rightarrow \infty$. Recall that every “hat” quantity ($\hat{F}_{i|y}$, $\hat{f}_{i|y}$, \tilde{c}_y , \hat{p}_y , \hat{Y} , etc.) depends on the total sample size n because it is estimated from n i.i.d. training pairs.

Step 1: Marginal Convergence By Assumption 4.4(5),

$$\sup_{x \in \mathbb{R}} |\hat{F}_{i|y}(x) - F_{i|y}(x)| = O_p(n^{-\alpha}), \quad \alpha > \frac{r}{2r+d}.$$

Define, for each training point X_i ,

$$u_i = F_{i|y}(X_i), \quad \hat{u}_i = \hat{F}_{i|y}(X_i).$$

Then directly,

$$|\hat{u}_i - u_i| = |\hat{F}_{i|y}(X_i) - F_{i|y}(X_i)| \leq \sup_x |\hat{F}_{i|y}(x) - F_{i|y}(x)| = O_p(n^{-\alpha}).$$

Therefore the vector of pseudo-observations $\hat{\mathbf{u}} = (\hat{u}_1, \dots, \hat{u}_d)$ satisfies

$$\|\hat{\mathbf{u}} - \mathbf{u}\|_\infty = O_p(n^{-\alpha}).$$

(Assumption 4.4(2) gives local bi-Lipschitz behavior away from boundaries; standard Winsorization/monotone smoothing near the boundary keeps rates unchanged.)

Step 2: Neural Copula Approximation Assumption 4.4(3) guarantees that our chosen class of neural networks can approximate any Sobolev-smooth copula density. In particular, since the true class-conditional copula $c_y \in W_2^r([0, 1]^d)$ with $r > d/2$, Schmidt-Hieber (2020) shows there exists a ReLU network of depth $O(\log n)$ and width $O(n^{d/(2r+d)})$ whose parameters θ_y^* satisfy

$$\sup_{u \in [0,1]^d} |NN_y(u; \theta_y^*) - c_y(u)| = O(n^{-r/(2r+d)}).$$

Let $\tilde{c}_y(u) = \frac{NN_y(u; \hat{\theta}_y)}{\hat{Z}_y(\hat{\theta}_y)}$ denote the normalized network after training on n_y samples, with $\hat{Z}_y(\hat{\theta}_y) = \frac{1}{M} \sum_{m=1}^M NN_y(V^{(m)}; \hat{\theta}_y)$.

By standard Rademacher-complexity-based MLE arguments (Koltchinskii (2001)), one shows

$$\mathbb{E}_{u \sim \text{Unif}[0,1]^d} [|NN_y(u; \hat{\theta}_y) - c_y(u)|^2] = O_p\left(n^{-\frac{2r}{2r+d}} + n^{-1}\right).$$

Passing to the normalized estimator $\tilde{c}_y(u) = NN_y(u; \hat{\theta}_y) / \hat{Z}_y(\hat{\theta}_y)$, write

$$\tilde{c}_y(u) - c_y(u) = \frac{NN_y(u; \hat{\theta}_y) - c_y(u)}{\hat{Z}_y(\hat{\theta}_y)} + c_y(u) \left(\frac{1}{\hat{Z}_y(\hat{\theta}_y)} - 1 \right).$$

Hence

$$\|\tilde{c}_y - c_y\|_\infty \leq \|NN_y(\cdot; \hat{\theta}_y) - c_y\|_\infty \cdot |1/\hat{Z}_y| + \|c_y\|_\infty \cdot |1/\hat{Z}_y - 1|.$$

By the approximation and estimation bounds above, $\|NN_y - c_y\|_\infty = O_p(n^{-r/(2r+d)})$ (up to logs). Moreover, $\hat{Z}_y(\hat{\theta}_y) = \int NN_y + O_p(M^{-1/2})$ and $\int NN_y = 1 + O_p(n^{-r/(2r+d)})$ because NN_y uniformly approximates c_y and $\int c_y = 1$. Thus $|\hat{Z}_y - 1| = O_p(n^{-r/(2r+d)}) + O_p(M^{-1/2})$, so choosing M as in Assumption (6) yields

$$\|\tilde{c}_y - c_y\|_\infty = O_p(n^{-r/(2r+d)}).$$

Step 3: Decision Rule Stability For any test input $x = (x_1, \dots, x_d)$, define

$$p_y(\mathbf{x}) = c_y(F_{1|y}(x_1), \dots, F_{d|y}(x_d)) \times \prod_{i=1}^d f_{i|y}(x_i),$$

and its estimate

$$\hat{p}_y(\mathbf{x}) = \tilde{c}_y(\hat{\mathbf{u}}) \times \prod_{i=1}^d \hat{f}_{i|y}(x_i), \quad \text{where } \hat{\mathbf{u}} = (\hat{u}_1, \dots, \hat{u}_d).$$

We bound

$$\begin{aligned} |\hat{p}_y(\mathbf{x}) - p_y(\mathbf{x})| &= \left| \tilde{c}_y(\hat{\mathbf{u}}) \prod_{i=1}^d \hat{f}_{i|y}(x_i) - c_y(\mathbf{u}) \prod_{i=1}^d f_{i|y}(x_i) \right| \\ &\leq \underbrace{|\tilde{c}_y(\hat{\mathbf{u}}) - c_y(\mathbf{u})| \prod_{i=1}^d \hat{f}_{i|y}(x_i)}_{\text{(A) Copula-error}} + \underbrace{|c_y(\mathbf{u})| \left| \prod_{i=1}^d \hat{f}_{i|y}(x_i) - \prod_{i=1}^d f_{i|y}(x_i) \right|}_{\text{(B) Marginal-error}}. \end{aligned}$$

(A) Copula-error. Observe

$$|\tilde{c}_y(\hat{\mathbf{u}}) - c_y(\mathbf{u})| \leq |\tilde{c}_y(\hat{\mathbf{u}}) - c_y(\hat{\mathbf{u}})| + |c_y(\hat{\mathbf{u}}) - c_y(\mathbf{u})|.$$

1. From Step 2, $\sup_u |\tilde{c}_y(u) - c_y(u)| = O_p(n^{-r/(2r+d)})$. 2. By Assumption (3), c_y is Lipschitz continuous on $[0, 1]^d$. Let L_c denote its Lipschitz constant. Then

$$|c_y(\hat{\mathbf{u}}) - c_y(\mathbf{u})| \leq L_c \|\hat{\mathbf{u}} - \mathbf{u}\|_\infty = O_p(n^{-\alpha}) \quad (\text{from Step 1}).$$

Hence

$$\sup_x |\tilde{c}_y(\hat{\mathbf{u}}) - c_y(\mathbf{u})| = O_p(n^{-\frac{r}{2r+d}} + n^{-\alpha}).$$

Since each $\hat{f}_{i|y}(x_i)$ is $O_p(1)$ uniformly (Assumption 4.4(2)), it follows that

$$\sup_x |\tilde{c}_y(\hat{\mathbf{u}}) - c_y(\mathbf{u})| \prod_i \hat{f}_{i|y}(x_i) = O_p(n^{-\frac{r}{2r+d}} + n^{-\alpha}).$$

(B) Marginal-error. Write $g_i(x_i) = f_{i|y}(x_i)$ and $\hat{g}_i(x_i) = \hat{f}_{i|y}(x_i)$. Then

$$\prod_{i=1}^d \hat{g}_i(x_i) - \prod_{i=1}^d g_i(x_i) = \sum_{j=1}^d (\hat{g}_j(x_j) - g_j(x_j)) \prod_{i < j} \hat{g}_i(x_i) \prod_{i > j} g_i(x_i).$$

By Step 1 and standard kernel-density theory (Silverman, 1986; Wasserman, 2006), $\sup_{x_i} |\hat{g}_i(x_i) - g_i(x_i)| = O_p(n^{-\alpha})$. Since each \hat{g}_i and g_i is bounded in probability by some constant M , each summand is

$$O_p(n^{-\alpha}) \times M^{d-1} = O_p(n^{-\alpha}).$$

Because there are d terms,

$$\sup_x \left| \prod_{i=1}^d \hat{g}_i(x_i) - \prod_{i=1}^d g_i(x_i) \right| = O_p(n^{-\alpha}).$$

Since $c_y(\mathbf{u})$ is bounded by Sobolev embedding, it follows that

$$\sup_x \left| c_y(\mathbf{u}) \left(\prod_i \hat{f}_{i|y}(x_i) - \prod_i f_{i|y}(x_i) \right) \right| = O_p(n^{-\alpha}).$$

Putting (A) and (B) Together Combining the bounds for (A) and (B) gives

$$\sup_x |\hat{p}_y(\mathbf{x}) - p_y(\mathbf{x})| = O_p(n^{-\frac{r}{2r+d}} + n^{-\alpha}).$$

Since $\alpha > \frac{r}{2r+d}$ by Assumption 4.4(5), the term $n^{-\alpha}$ is asymptotically smaller, so

$$\sup_x |\hat{p}_y(\mathbf{x}) - p_y(\mathbf{x})| = O_p(n^{-\frac{r}{2r+d}}).$$

The classifier uses the joint distribution $\hat{\pi}_y \hat{p}_y(\mathbf{x})$. Given the consistent estimation of the prior ($\hat{\pi}_y \rightarrow \pi_y$) and the uniform convergence of the density, we have:

$$\arg \max_y \hat{\pi}_y \hat{p}_y(\mathbf{x}) \xrightarrow{P} \arg \max_y \pi_y p_y(\mathbf{x}).$$

by a standard argmax-continuity argument (e.g., Portmanteau lemma [van der Vaart \(2012\)](#) plus union bound over the finitely many classes). Therefore \hat{Y} converges in probability to the Bayes-optimal decision Y^* . This completes the proof of Theorem 1.

A.3 Proof of Theorem 2 (Convergence Rate)

We now show that, under the same regularity assumptions plus $c_y \in W_2^r([0, 1]^d)$, the excess classification risk decays at rate $n^{-r/(2r+d)}$.

Define

$$E(n) = \mathbb{P}(\hat{Y}_n(\mathbf{X}) \neq Y) - \mathbb{P}(Y^*(\mathbf{x}) \neq Y), \quad Y^*(\mathbf{x}) = \arg \max_y \pi_y p_y(\mathbf{x}).$$

By Lemma A.1, the plug-in regret is controlled by the L^1 error of the class-conditional joints.

Hence,

$$E(n) \leq \sum_{y=1}^K \|\hat{\pi}_y \hat{p}_y - \pi_y p_y\|_1 = O_p(n^{-r/(2r+d)}),$$

since $|\hat{\pi}_y - \pi_y| = O_p(n^{-1/2})$ and $\|\hat{p}_y - p_y\|_1 = O_p(n^{-r/(2r+d)})$.

1. **Copula-Approximation Error:** By [Schmidt-Hieber \(2020\)](#), there exists a ReLU network of depth $O(\log n)$, width $O(n^{d/(2r+d)})$, and parameters θ_y^* such that

$$\inf_{\theta} \|NN_y(\cdot; \theta) - c_y\|_{L^2([0,1]^d)} \leq C n^{-r/(2r+d)}.$$

Sobolev embedding (since $r > d/2$) implies

$$\sup_{u \in [0,1]^d} |NN_y(u; \theta_y^*) - c_y(u)| = O(n^{-r/(2r+d)}).$$

Consequently,

$$\|NN_y(\cdot; \theta_y^*) \prod_i f_{i|y} - c_y \prod_i f_{i|y}\|_{L^1} = O(n^{-r/(2r+d)}), \quad \left(\int \prod_i f_{i|y} = 1 \right).$$

2. Network-Estimation Error. Let

$$\mathcal{F}_{y,n} = \{ u \mapsto NN_y(u; \theta) : \theta \text{ ranges over all ReLU-networks of depth } L_n = O(\log n) \text{ and width } W_n = O(n^{d/(2r+d)}) \}.$$

We train $\hat{\theta}_y$ by maximizing the normalized log-likelihood of $u \mapsto \frac{NN_y(u; \theta)}{\hat{Z}_y(\theta)}$ on the n_y “pseudo-observations” $\{ u^{(i)} = \hat{\mathbf{u}}^{(i)} \mid y^{(i)} = y \}$, each distributed roughly like $\text{Unif}[0, 1]^d$.

In [Farrell, Liang and Misra \(2021\)](#), it is shown that if a function class \mathcal{F} has Gaussian-complexity (or Rademacher-complexity) bounded by $\mathfrak{R}(n)$, then the empirical-risk minimizer \hat{f} over \mathcal{F} satisfies with probability at least $1 - \delta$:

$$\mathbb{E}_{u \sim \text{Unif}[0,1]^d} [|\hat{f}(u) - c_y(u)|^2] \leq \inf_{f \in \mathcal{F}} \mathbb{E}_u [|f(u) - c_y(u)|^2] + O(\mathfrak{R}(n)) + O(n^{-1}).$$

In our setting:

- The *approximation bias* $\inf_{\theta} \mathbb{E}_u [|NN_y(u; \theta) - c_y(u)|^2]$ is already $O(n^{-2r/(2r+d)})$ by the same Sobolev-approximation argument of Schmidt–Hieber (since $\sup_u |NN_y(u; \theta_y^*) - c_y(u)| = O(n^{-r/(2r+d)})$, and thus its L^2 -norm is $O(n^{-2r/(2r+d)})$).
- The *Gaussian complexity* $\mathfrak{R}(n)$ of $\mathcal{F}_{y,n}$ can be bounded by

$$\mathfrak{R}(n) \approx O\left(\sqrt{\frac{L_n W_n}{n}}\right) = O\left(\sqrt{\frac{(\log n) n^{d/(2r+d)}}{n}}\right) = O\left(n^{-\frac{r}{2r+d}}\right),$$

up to logarithmic factors. Concretely, standard covering-number or Rademacher-complexity bounds for ReLU networks ([Bartlett and Mendelson \(2002\)](#); [Koltchinskii \(2001\)](#)) show that

$$\mathfrak{R}(n) = O\left(\sqrt{\frac{LW}{n}}\right) \text{ whenever } L = O(\log n), W = O(n^{d/(2r+d)}).$$

Hence $\mathfrak{R}(n) = O(n^{-r/(2r+d)})$.

Therefore, from [Farrell, Liang and Misra \(2021\)](#) with $\inf_{f \in \mathcal{F}_{y,n}} \mathbb{E}[|f(u) - c_y(u)|^2] = O(n^{-2r/(2r+d)})$ and $\mathfrak{R}(n) = O(n^{-r/(2r+d)})$, we get, *with probability at least* $1 - \delta$, that

$$\mathbb{E}_u [|NN_y(u; \hat{\theta}_y) - c_y(u)|^2] = O\left(n^{-\frac{2r}{2r+d}}\right) + O\left(n^{-\frac{r}{2r+d}}\right) + O(n^{-1}).$$

Since $r > d/2$, the largest of these exponents is $\frac{2r}{2r+d} > \frac{r}{2r+d}$. In big- O notation, one thus writes

$$\mathbb{E}_u [|NN_y(u; \hat{\theta}_y) - c_y(u)|^2] = O_p\left(n^{-\frac{2r}{2r+d}} + n^{-1}\right).$$

Finally, because $c_y \in W_2^r([0, 1]^d)$ with $r > d/2$, Sobolev-embedding guarantees an $L^2 \rightarrow L^\infty$ upgrade (up to logs):

$$\sup_{u \in [0,1]^d} |\tilde{c}_y(u) - c_y(u)| = O_p(n^{-r/(2r+d)}).$$

Hence overall

$$\|\tilde{c}_y(\cdot) \prod_i f_{i|y} - c_y \prod_i f_{i|y}\|_{L^1} = O_p(n^{-r/(2r+d)}).$$

3. **Marginal-Estimation Error:** Under the regularity conditions in Section 4.4(5),

$$\sup_{x_i} |\widehat{F}_{i|y}(x_i) - F_{i|y}(x_i)| = O_p(n^{-\alpha}), \quad \alpha > \frac{r}{2r+d}.$$

By standard kernel-density theory (Silverman, 1986; Wasserman, 2006), $\sup_{x_i} |\widehat{f}_{i|y}(x_i) - f_{i|y}(x_i)| = O_p(n^{-\alpha})$. Since each $f_{i|y}$ is bounded away from zero and infinity on its compact support (Assumption 2), a telescoping product-difference argument shows

$$\sup_x \left| \prod_{i=1}^d \widehat{f}_{i|y}(x_i) - \prod_{i=1}^d f_{i|y}(x_i) \right| = O_p(n^{-\alpha}).$$

Moreover, c_y is bounded by Sobolev embedding, so

$$\left\| c_y \left(\prod_i \widehat{f}_{i|y} - \prod_i f_{i|y} \right) \right\|_{L^1} = O_p(n^{-\alpha}).$$

Combining 1,2 and 3, we conclude for each class y :

$$\|\widehat{p}_y - p_y\|_{L^1} = O_p(n^{-r/(2r+d)} + n^{-\alpha}) = O_p(n^{-r/(2r+d)}),$$

since $\alpha > r/(2r+d)$. Therefore, the dominant term in the excess risk bound is:

$$E(n) = C \sum_{y=1}^K \|\widehat{p}_y - p_y\|_{L^1} + O_p(n^{-1/2}) = O_p(n^{-r/(2r+d)}).$$

This completes the proof of Theorem 2.

Remark. Any extra $\log n$ or $\log(1/\delta)$ factors from covering-number or union-bound arguments are absorbed into the $O_p(\cdot)$ notation and do not affect the leading exponent $r/(2r+d)$.

A.4 Proof of Proposition 4.1 (Asymptotic copula validity)

Fix a class y and drop the subscript for readability. Let

$$\ell_n(\theta) = \frac{1}{n_y} \sum_{i: Y^{(i)}=y} \log \tilde{c}(\widehat{u}^{(i)}; \theta), \quad D(\theta) = \sum_{i=1}^d \int_0^1 \left(\int \tilde{c}(u; \theta) du_{-i} - 1 \right)^2 du_i,$$

and define the empirical penalized criterion $Q_n(\theta) = \ell_n(\theta) - \lambda_n D(\theta)$ with maximizer $\hat{\theta} \in \arg \max_{\theta} Q_n(\theta)$. We prove $D(\hat{\theta}) \xrightarrow{p} 0$.

Step 1 (Empirical PIT vs. true PIT). Let $u^{(i)} = F(X^{(i)})$ be the true PIT and $\widehat{u}^{(i)} = \widehat{F}(X^{(i)})$ the empirical/smoothed PIT used in training. By Assumption 4.4(5a), $\|\widehat{F} - F\|_{\infty} = O_p(n_y^{-1/2})$; since $\log \tilde{c}(\cdot; \theta)$ is uniformly Lipschitz on $[0, 1]^d$ under the spectral/weight regularization of Section 5.3, we have

$$\sup_{\theta} |\ell_n(\theta) - \tilde{\ell}_n(\theta)| = o_p(1), \quad \tilde{\ell}_n(\theta) = \frac{1}{n_y} \sum_{i: y} \log \tilde{c}(u^{(i)}; \theta).$$

Thus we can work with true PITs without changing maximizers asymptotically.

Step 2 (MC normalizer is uniformly accurate). Write $Z(\theta) = \int_{[0,1]^d} NN(v; \theta) dv$ and $\widehat{Z}(\theta) = (1/M) \sum_{m=1}^M NN(V^{(m)}; \theta)$ with $V^{(m)} \sim \text{Unif}([0, 1]^d)$ i.i.d. By standard empirical process bounds for bounded Lipschitz network classes (covering numbers of ReLU nets with spectral bounds),

$$\sup_{\theta} |\widehat{Z}(\theta) - Z(\theta)| = O_p\left(\sqrt{\frac{C_n}{M}}\right),$$

where C_n is a complexity term polynomial in the network size S_n (hidden in u.c.b.). By Assumption 4.4 (6), $M^{-1/2} = o(n^{-r/(2r+d)})$, hence $\sup_{\theta} |\log \widehat{Z}(\theta) - \log Z(\theta)| = o_p(1)$ and

$$\sup_{\theta} \left| \log \tilde{c}(u; \theta) - (\log NN(u; \theta) - \log Z(\theta)) \right| = o_p(1) \quad \text{uniformly in } u.$$

Consequently, $\sup_{\theta} |\tilde{\ell}_n(\theta) - \bar{\ell}_n(\theta)| = o_p(1)$ with $\bar{\ell}_n(\theta) = \frac{1}{n_y} \sum_i (\log NN(u^{(i)}; \theta) - \log Z(\theta))$.

Step 3 (Uniform LLN and the population criterion). Let $\ell(\theta) = \mathbb{E}[\log \tilde{c}(U; \theta)]$ with $U \sim c$ the true copula. The class $\{\log \tilde{c}(\cdot; \theta) : \theta \in \Theta_n\}$ is Glivenko–Cantelli under the same complexity control (bounded outputs/Lipschitz + growing S_n per Assumption 4.4 (3)), so $\sup_{\theta} |\tilde{\ell}_n(\theta) - \ell(\theta)| = o_p(1)$. Define the population penalized functional

$$Q(\theta) = \ell(\theta) - \lambda_n D(\theta).$$

Note $\ell(\theta) = \text{const} - \text{KL}(c \parallel \tilde{c}(\cdot; \theta))$; thus, for any density candidate g on $[0, 1]^d$, $\ell(g) \leq \ell(c)$ with equality iff $g = c$ a.e.

Step 4 (There exist near-copula approximants in the model class). By Assumption 4.4 (3), for any $\varepsilon > 0$ there is θ_ε such that $\|NN(\cdot; \theta_\varepsilon) - c\|_1 \leq \varepsilon$. After normalization, $\|\tilde{c}(\cdot; \theta_\varepsilon) - c\|_1 \leq C\varepsilon$. Fubini's theorem gives, for each margin i ,

$$\sup_{u_i \in [0,1]} \left| \int \tilde{c}(u; \theta_\varepsilon) du_{-i} - 1 \right| \leq \|\tilde{c}(\cdot; \theta_\varepsilon) - c\|_1 \leq C\varepsilon,$$

so $D(\theta_\varepsilon) \leq C\varepsilon^2$ and $\ell(\theta_\varepsilon) \geq \ell(c) - C\varepsilon$. Choosing a sequence $\varepsilon = \varepsilon_n \downarrow 0$ and corresponding θ_n° in the growing class (size S_n) yields

$$\ell(\theta_n^\circ) = \ell(c) - o(1), \quad D(\theta_n^\circ) = o(1).$$

Step 5 (Penalty forces the defect to zero). By optimality of $\hat{\theta}$ for Q_n and the uniform $o_p(1)$ approximations from Steps 0–2,

$$\ell(\hat{\theta}) - \lambda_n D(\hat{\theta}) \geq \ell(\theta_n^\circ) - \lambda_n D(\theta_n^\circ) - o_p(1).$$

Rearrange:

$$\lambda_n (D(\hat{\theta}) - D(\theta_n^\circ)) \leq \ell(\hat{\theta}) - \ell(\theta_n^\circ) + o_p(1).$$

The RHS is $O_p(1)$ uniformly (both terms are bounded by u.c.b.), hence

$$D(\hat{\theta}) \leq D(\theta_n^\circ) + O_p(\lambda_n^{-1}) = o_p(1)$$

because $D(\theta_n^\circ) = o(1)$ and $\lambda_n \rightarrow \infty$. This proves the first claim.

Step 6 (Rate compatibility). Since $D(\hat{\theta}) = o_p(1)$ and $\tilde{c}(\cdot; \hat{\theta})$ remains in a uniformly bounded Lipschitz ball (spectral control), the marginal-uniformity error contributes at most $o_p(n^{-r/(2r+d)})$ to the density sup-norm error by the same linear functional bound as in Step 3; thus it does not change the dominant classification rate $n^{-r/(2r+d)}$ used in Theorem 2. \square

A.5 Proof of Corollary 4.1 (Fast excess-risk under a multiclass margin)

Recall $a_y(x) = \pi_y p_y(x)$, $\hat{a}_y(x) = \hat{\pi}_y \hat{p}_y(x)$, $\eta_y(x) = a_y(x)/A(x)$ with $A(x) = \sum_{k=1}^K a_k(x) = p_X(x)$, and likewise $\hat{\eta}_y(x) = \hat{a}_y(x)/\hat{A}(x)$ with $\hat{A} = \sum_k \hat{a}_k$. Write $\varepsilon(x) = \max_{y \in [K]} |\hat{\eta}_y(x) - \eta_y(x)|$ and $\Delta(x) = \eta_{(1)}(x) - \eta_{(2)}(x)$.

Step 1 (From joint-density error to conditional-probability error in $L^1(P_X)$). For every x and y ,

$$A(x) |\hat{\eta}_y(x) - \eta_y(x)| = \left| \hat{a}_y(x) - a_y(x) - \eta_y(x)(\hat{A}(x) - A(x)) \right| \leq \sum_{k=1}^K |\hat{a}_k(x) - a_k(x)|.$$

Taking \max_y and integrating over \mathbb{R}^d ,

$$\int \varepsilon(x) dP_X(x) = \int A(x) \varepsilon(x) dx \leq K \sum_{k=1}^K \int |\hat{a}_k(x) - a_k(x)| dx.$$

By Theorem 2 and $|\hat{\pi}_k - \pi_k| = O_p(n^{-1/2})$, $\sum_k \|\hat{a}_k - a_k\|_{L^1} = O_p(n^{-\frac{r}{2r+d}})$. Hence

$$\|\hat{\eta} - \eta\|_{L^1(P_X)} = \mathbb{E}[\varepsilon(X)] = O_p(n^{-\frac{r}{2r+d}}). \quad (2)$$

Step 2 (Uniform control on the effective support). Let S_n be the set from Assumption 4.4 with $P_X(S_n) \rightarrow 1$ and $\inf_{x \in S_n} A(x) \geq c_0 > 0$. For $x \in S_n$ and any y ,

$$|\hat{\eta}_y(x) - \eta_y(x)| \leq \frac{1}{A(x)} \sum_{k=1}^K |\hat{a}_k(x) - a_k(x)| \leq \frac{1}{c_0} \sum_{k=1}^K |\hat{a}_k(x) - a_k(x)|.$$

By the uniform bound established in the proof of Theorem 2, $\sup_x |\hat{p}_k(x) - p_k(x)| = O_p(n^{-\frac{r}{2r+d}})$ (up to logs), and $|\hat{\pi}_k - \pi_k| = O_p(n^{-1/2})$, hence

$$\sup_{x \in S_n} \varepsilon(x) = O_p(n^{-\frac{r}{2r+d}}).$$

The contribution from S_n^c is negligible since $P_X(S_n^c) \rightarrow 0$ and $\varepsilon \leq 2$.

Step 3 (Margin transfer: excess risk vs. ε). Let \hat{Y} be the plug-in classifier and Y^* the Bayes rule. A standard argument (e.g., Audibert–Tsybakov, 2007; multiclass reduction to top-two comparison) yields

$$R(\hat{Y}) - R(Y^*) \leq C_1 \mathbb{E}[\varepsilon(X)^{1+\kappa}],$$

whenever the multiclass Tsybakov margin condition $P(\Delta(X) \leq t) \leq Ct^\kappa$ holds.

Step 4 (Putting the bounds together). On S_n , $\varepsilon(X) \leq C_2 n^{-\frac{r}{2r+d}}$ with probability $1-o(1)$. Thus $\mathbb{E}[\varepsilon(X)^{1+\kappa} \mathbf{1}_{S_n}] \leq C_2^{1+\kappa} n^{-\frac{(1+\kappa)r}{2r+d}}$. On S_n^c , $\varepsilon \leq 2$ and $P_X(S_n^c) = o(1)$, so $\mathbb{E}[\varepsilon^{1+\kappa} \mathbf{1}_{S_n^c}] = o(1) \cdot 2^{1+\kappa}$. Therefore,

$$R(\hat{Y}) - R(Y^*) = O_p\left(n^{-\frac{(1+\kappa)r}{2r+d}}\right). \quad \square$$